

Spatial-Temporal Large Language Model for Traffic Prediction

Chenxi Liu¹, Sun Yang², Qianxiong Xu¹, Zhishuai Li³, Cheng Long¹, Ziyue Li⁴, Rui Zhao³

¹S-Lab, Nanyang Technological University

²Peking University

³SenseTime Research

⁴Information System Department, University of Cologne

{chenxi.liu, qianxiong.xu, c.long}@ntu.edu.sg, {lizhishuai, zhaorui}@sensetime.com,
2201210484@stu.pku.edu.cn, zlibn@wiso.uni-koeln.de

Abstract

Traffic prediction, a critical component for intelligent transportation systems, endeavors to foresee future traffic at specific locations using historical data. Although existing traffic prediction models often emphasize developing complex neural network structures, their accuracy has not seen improvements accordingly. Recently, Large Language Models (LLMs) have shown outstanding capabilities in time series analysis. Differing from existing models, LLMs progress mainly through parameter expansion and extensive pre-training while maintaining their fundamental structures. In this paper, we propose a Spatial-Temporal Large Language Model (ST-LLM) for traffic prediction. Specifically, ST-LLM redefines the timesteps at each location as tokens and incorporates a spatial-temporal embedding module to learn the spatial location and global temporal representations of tokens. Then these representations are fused to provide each token with unified spatial and temporal information. Furthermore, we propose a novel partially frozen attention strategy of the LLM, which is designed to capture spatial-temporal dependencies for traffic prediction. Comprehensive experiments on real traffic datasets offer evidence that ST-LLM outperforms state-of-the-art models. Notably, the ST-LLM also exhibits robust performance in both few-shot and zero-shot prediction scenarios.

1 Introduction

Traffic prediction, which aims to predict future traffic features like flow at specific locations using historical data, is a crucial component for intelligent transportation systems [Li *et al.*, 2023; Jiang *et al.*, 2023; Chang *et al.*, 2023; Li *et al.*, 2023; Gong *et al.*, 2023]. This prediction is instrumental in optimizing traffic management [Miao *et al.*, 2024; Zhou *et al.*, 2024] and scheduling public transportation [Jin *et al.*, 2023a; Wang *et al.*, 2020]. For instance, accurately predicting bike flow benefits the transportation department in optimizing bike management. Similarly, taxi flow forecasting is vital for vehicle companies, as it enables them to efficiently allocate and schedule vehicles to satisfy expected demand.

The evolution of traffic prediction has seen a shift from traditional time series models to deep learning techniques [Campos *et al.*, 2023; Chang *et al.*, 2023; Yuan *et al.*, 2018; Kumar and Vanajakshi, 2015]. Initially, time series models such as the Autoregressive Integrated Moving Average and Kalman Filter were adapted for their fit with time series data. However, these models are not good at capturing the spatial-temporal dependencies within traffic data, leading to deep learning solutions using convolutional neural networks (CNNs) for spatial and recurrent neural networks (RNNs) for temporal dependencies [Yin *et al.*, 2021; Shen *et al.*, 2018; Yuan *et al.*, 2018]. Despite these advancements, the non-Euclidean spatial structure and the complex periodicity of traffic data present challenges for CNNs and RNNs in capturing spatial and temporal dependencies well.

Graph convolutional network (GCN) based models gained popularity for their ability to model local spatial dependencies [Li *et al.*, 2023; Bai *et al.*, 2020; Bai *et al.*, 2020; Wu *et al.*, 2019; Li *et al.*, 2018; Yu *et al.*, 2018]. However, these models often encountered over-smoothing issues, which limits their ability to capture global spatial patterns. This shortcoming prompted a shift to attention-based models, which effectively model dynamic spatial correlations without depending on an adjacency matrix [Jiang *et al.*, 2023; Guo *et al.*, 2022; Lin *et al.*, 2020]. These attention-based approaches have since emerged as a leading trend, offering a superior ability of handling spatial-temporal dependencies in traffic prediction [Zheng *et al.*, 2020; Guo *et al.*, 2019]. Nevertheless, with this evolution, the structures of existing traffic prediction models have become progressively complex.

Foundation models, including large language models (LLMs), have advancements in fields such as computer vision [Ko *et al.*, 2023; Yu *et al.*, 2023] and natural language processing [Ramezani and Xu, 2023; Maynez *et al.*, 2023]. More recently, LLMs also have shown superb performance on time series analysis [Cao *et al.*, 2023; Jin *et al.*, 2023b]. Compared with the complex designs of existing predictive models, LLMs primarily evolve through the expansion of parameters and pre-training while maintaining their foundational model structure. Existing LLM-based prediction methods tend to focus on the temporal aspect of data in the traffic prediction tasks [Zhou *et al.*, 2023; Jin *et al.*, 2023b; Cao *et al.*, 2023] and often overlook the spatial aspect. However, in traffic prediction, the spatial variables are strongly

correlated and the spatial dimension also proves to be important [Lablack and Shen, 2023; Wen *et al.*, 2023]. For example, a common problem setting is to use traffic data from the previous *twelve* timesteps to predict traffic for the next *twelve* timesteps at *hundreds* of spatial locations [Li *et al.*, 2018] - in this case, more spatial data than temporal data can be leveraged. In our study, we refine the timesteps of a spatial location as a token and model the global temporal dependencies across all these tokens so as to emphasize the spatial aspects.

Moreover, LLMs are notable for their ability to transfer knowledge across domains [Rasul *et al.*, 2023; Nate Gruver and Wilson, 2023], such as the pretrained transformer (FPT) LLM [Zhou *et al.*, 2023]. While the FPT LLM is effective in time series analysis tasks, it shows less optimal performance in long-term prediction tasks like traffic prediction. The possible reason is that FPT struggles to bridge the domain gap between language data and traffic data. To fill this gap, we propose a partially frozen attention (PFA) LLM, specifically designed to enhance prediction accuracy in traffic prediction. By partially freezing the multi-head attention, the LLM can adapt to traffic prediction while preserving the foundational knowledge acquired during pre-training.

In summary, we propose a novel framework for traffic prediction termed Spatial-Temporal Large Language Model (ST-LLM). In this model, we define timesteps at a location as a token. These tokens transform a specialized spatial-temporal embedding layer, which is designed to emphasize spatial and temporal correlations such as spatial correlations and temporal patterns. Furthermore, we fuse the spatial-temporal embeddings of each token. This fusion process plays a pivotal role in aggregating spatial and temporal embeddings into a unified representation. Following this, we introduce the partially frozen attention LLM, a novel strategy tailored for LLMs to effectively capture the spatial-temporal dependencies in traffic prediction. Extensive experiments on real-world traffic datasets have validated the efficacy of ST-LLM. The key contributions of this paper are summarized as follows:

- We propose a novel Spatial-Temporal Large Language Model (ST-LLM) for traffic prediction, which defines timesteps at a location as a token and embeds each token by a spatial-temporal embedding layer. We fuse the spatial-temporal embeddings of these tokens uniformly and adapt the LLMs for capturing global spatial-temporal dependencies.
- A novel strategy within the LLM, named partially frozen attention, is proposed to enhance the model in traffic prediction. By partially freezing the multi-head attention, the ST-LLM is adapted to capture global spatial-temporal dependencies between tokens for different traffic prediction tasks.
- Extensive experiments are conducted on real traffic datasets to show the superior performance achieved by our ST-LLM across various settings. Moreover, the few-shot and zero-shot prediction results highlight the ST-LLM’s capability for intra-domain and inter-domain knowledge transfer.

2 Related Work

2.1 Large Language Models for Time Series Analysis

Recently large language models (LLMs) have shown superb performance on time series analysis tasks, such as prediction [Cao *et al.*, 2023], classification [Jin *et al.*, 2023b], anomaly detection [Zhou *et al.*, 2023], imputation [Chen *et al.*, 2023], few-shot learning [Sun *et al.*, 2023], and zero-shot learning [Nate Gruver and Wilson, 2023]. For instance, TEMPO-GPT combines prompt engineering and seasonal trend decomposition in the generative pre-trained transformer (GPT) [Cao *et al.*, 2023]. TIME-LLM reprograms an LLM for time series forecasting, and the backbone language model remains intact [Jin *et al.*, 2023b]. OFA employs a frozen GPT2 model across various key tasks in time series analysis [Zhou *et al.*, 2023], the authors conclude that the LLM performs better on tasks of time series analysis. TEST generates various embedding for time series tokens and executes time series forecasting and classification tasks [Sun *et al.*, 2023]. The above model only models the temporal dimension of the data and ignores the spatial dimension. GATGPT integrates the graph attention network and GPT for spatial-temporal imputation [Chen *et al.*, 2023]. However, it directly overlooks the temporal representation. As of now, the technique for effectively embedding time series data that encompasses both spatial and temporal representations before inputting it into LLMs is not well-defined.

2.2 Traffic Prediction

Traffic prediction aims to predict future traffic features based on historical traffic data, which is crucial for intelligent transportation systems [Ye *et al.*, 2021; Shao *et al.*, 2022; Miao *et al.*, 2023]. Traditionally, the traffic prediction model is based on statistics, such as ARIMA and Kalman filter [Kumar and Vanajakshi, 2015; Chang *et al.*, 2023]. However, these models do not perform well due to the inherent spatial-temporal dependencies of traffic data. Later, numerous efforts have been dedicated to advancing traffic prediction techniques through the development of various neural network-based models. First, convolutional neural networks (CNNs) were applied to traffic data to capture spatial dependencies in the data [Shen *et al.*, 2018; Yuan *et al.*, 2018]. Given that CNNs are primarily designed for regular, grid-like urban areas, they encounter challenges when dealing with the non-Euclidean spatial structure of traffic data. Then, graph convolutional network (GCN) based models became popular due to their permutation-invariance, local connectivity, and compositionality [Wu *et al.*, 2019; Bai *et al.*, 2020]. More recently, attention-based models have emerged as a dominant trend [Guo *et al.*, 2019; Zheng *et al.*, 2020; Guo *et al.*, 2022; Jiang *et al.*, 2023]. Without taking the adjacency matrix into account, attention-based models can still model dynamic spatial correlation more effectively than GCN-based models [Liu *et al.*, 2023a]. However, the structures of these models are becoming increasingly sophisticated.

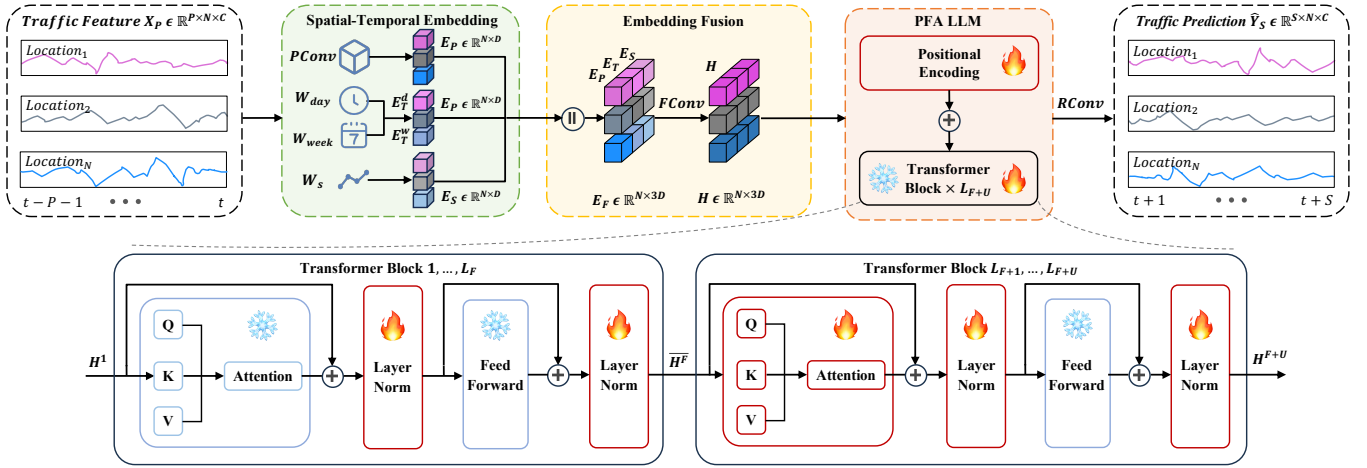


Figure 1: ST-LLM framework. Given an input traffic feature, we first embed it via a **Spatial-Temporal Embedding**. These embeddings are then integrated uniformly by an **Embedding Fusion** layer. The **PFA (partially frozen attention) LLM** has $F + U$ layers, which are divided into the first F layers and the last U layers. The multi-head attention and feed-forward layers in the first F layers are frozen, and the multi-head attention in the last U layers are unfrozen. The output from PFA LLM is regressed to the prediction results.

3 Problem Definition

Definition 3.1 (Traffic Feature). We denote the traffic data as a tensor $\mathbf{X} \in \mathbb{R}^{T \times N \times C}$, where T is the number of timesteps, N is the number of spatial stations, and C is the feature. For example, $C = 1$ represents the traffic pick-up or drop-off flow.

Definition 3.2 (Traffic Prediction). Given the historical traffic feature of P timesteps $\mathbf{X}_P = \{\mathbf{X}_{t-P+1}, \mathbf{X}_{t-P+2}, \dots, \mathbf{X}_t\} \in \mathbb{R}^{P \times N \times C}$, the objective is to learn a function $f(\cdot)$ with parameter θ to predict traffic feature of on the following S timesteps $\mathbf{Y}_S = \{\mathbf{Y}_{t+1}, \mathbf{Y}_{t+2}, \dots, \mathbf{Y}_{t+S}\} \in \mathbb{R}^{S \times N \times C}$. That is,

$$[\mathbf{X}_{t-P+1}, \mathbf{X}_{t-P+2}, \dots, \mathbf{X}_t] \xrightarrow{\theta} [\mathbf{Y}_{t+1}, \mathbf{Y}_{t+2}, \dots, \mathbf{Y}_{t+S}], \quad (1)$$

where $\mathbf{X}_i \in \mathbb{R}^{N \times C}$.

4 Methodology

In this section, we provide a detailed elaboration of the proposed ST-LLM and its components.

4.1 Overview

The Spatial-Temporal Large Language Model (ST-LLM) framework, as depicted in Figure 1, integrates a spatial-temporal embedding layer, a fusion convolution layer, an LLM layer, and a regression convolution layer. Initially, the historical traffic data is denoted as \mathbf{X}_P , which contains N tokens of spatial locations. The \mathbf{X}_P is processed through the spatial-temporal embedding layer, which extracts the token embedding of historical P timestamps, spatial embedding, and temporal embedding, as $\mathbf{E}_T \in \mathbb{R}^{N \times D}$, $\mathbf{E}_S \in \mathbb{R}^{N \times D}$, and $\mathbf{E}_P \in \mathbb{R}^{N \times D}$, respectively. A fusion convolution then integrates these representations into a unified way $\mathbf{E}_F \in \mathbb{R}^{N \times 3D}$. Subsequently, the \mathbf{E}_F is input into a PFA LLM that encompasses $L + U$ layers, where the multi-head attention and feed forward layers in the first F layers are frozen to preserve the

pretrained knowledge and the multi-head attention layers in the last U layers are unfrozen to enhance the model’s focus on capturing the spatial-temporal dependencies between tokens, resulting in the output $\mathbf{H}^L \in \mathbb{R}^{N \times 3D}$. Finally, the regression convolution layer takes \mathbf{H}^L and predicts the following traffic data, denoted as $\hat{\mathbf{Y}}_S \in \mathbb{R}^{S \times N \times C}$.

4.2 Spatial-Temporal Embedding and Fusion

We aim to modify LLMs that have already been trained for traffic prediction tasks. We refine the timestamps at each location of traffic data as tokens. The spatial-temporal embedding layer is designed to transform the tokens into spatial-temporal representations that align with the LLMs. These representations including spatial correlations, hour-of-day, day-of-week patterns, and token information.

We embed the tokens through a pointwise convolution, where the input data \mathbf{X}_P is transformed into the embedding $\mathbf{E}_P \in \mathbb{R}^{N \times D}$:

$$\mathbf{E}_P = PConv(\mathbf{X}_P; \theta_p), \quad (2)$$

where \mathbf{E}_P represents the token embedding. $PConv$ denotes the pointwise convolution operation using filters that have a 1×1 kernel size. \mathbf{X}_P is the input data, D is the hidden dimension. θ_p represents the learnable parameters of the pointwise convolution.

To preserve the temporal information in the tokens, we utilize a linear layer to encode the input data into separate embeddings for the hour-of-day and day-of-week temporal embeddings. We perform absolute positional encoding for each traffic data at the “day” and “week” resolutions, and the generated positional encodings are $\mathbf{X}_{day} \in \mathbb{R}^{N \times T_d}$ and $\mathbf{X}_{week} \in \mathbb{R}^{N \times T_w}$. The hour-of-day embedding $\mathbf{E}_T^d \in \mathbb{R}^{N \times D}$ and day-of-week embedding $\mathbf{E}_T^w \in \mathbb{R}^{N \times D}$ are calculated as follows:

$$\mathbf{E}_T^d = \mathbf{W}_{day}(\mathbf{X}_{day}), \quad \mathbf{E}_T^w = \mathbf{W}_{week}(\mathbf{X}_{week}), \quad (3)$$

$\mathbf{W}_{day} \in \mathbb{R}^{T_d \times D}$ and $\mathbf{W}_{week} \in \mathbb{R}^{T_w \times D}$ are the learnable parameter embeddings for the hour-of-day and day-of-week, respectively. By adding these two embeddings, we obtain the temporal representation $\mathbf{E}_T \in \mathbb{R}^{N \times D}$.

To represent spatial correlations among token pairs, we design an adaptive embedding of tokens, $\mathbf{E}_S \in \mathbb{R}^{N \times D}$:

$$\mathbf{E}_S = \sigma(\mathbf{W}_s \cdot \mathbf{X}_P + \mathbf{b}_s), \quad (4)$$

where σ denotes the activation function, $\mathbf{W}_s \in \mathbb{R}^{D \times D}$ and $\mathbf{b}_s \in \mathbb{R}^D$ are the learnable parameter embeddings.

Subsequently, we introduce a fusion convolution (FConv) to integrate the token, spatial, and temporal embeddings to represent the spatial-temporal embedding of each token:

$$\mathbf{H}_F = FConv(\mathbf{E}_P || \mathbf{E}_S || \mathbf{E}_T; \theta_f), \quad (5)$$

where $\mathbf{H}_F \in \mathbb{R}^{N \times 3D}$, $||$ denotes concatenation, and θ_f represents the learnable parameters of the FConv.

4.3 Partially Frozen Attention (PFA) LLM

The frozen pretrained transformer (FPT) has demonstrated effectiveness in a variety of downstream tasks across non-language modalities [Lu *et al.*, 2022]. However, its performance is less optimal in tasks requiring both short-term and long-term predictions, such as traffic prediction [Zhou *et al.*, 2023]. To address this limitation, we propose a partially frozen attention (PFA) LLM, specifically designed to enhance prediction accuracy in traffic prediction.

The difference between the FPT and our PFA primarily lies in the configuration of frozen attention layers. In the FPT framework, both the multi-head attention and feed-forward layers are frozen during training, as these layers contain the most significant portion of the learned knowledge within the LLM. In the PFA, we maintain the first F layers identical to the FPT, but crucially, we unfreeze the last U multi-head attention layers since the attentions offer effective handling of spatial-temporal dependencies in data. Consequently, our ST-LLM can adapt to traffic prediction while preserving the foundational knowledge acquired during pre-training.

Furthermore, our ST-LLM inverts the traditional calculation dimension from temporal to spatial. This inversion is intentional and aligns with the operation of the partially frozen layers. By focusing on spatial dimensions, our model captures global correlations more effectively than if we were to concentrate solely on temporal aspects. This shift is particularly relevant in the context of traffic prediction, where spatial dynamics play a critical role in determining flow patterns.

To elaborate, the PFA LLM generates a probabilistic distribution of the new representations based on the sequence of existing embedded representations $\mathbf{H} =$

$\{\mathbf{H}^1, \mathbf{H}^2, \dots, \mathbf{H}^N\}$. In the first F layers of the LLM:

$$\begin{aligned} \bar{\mathbf{H}}^i &= LN(\mathbf{H}^i + MHA(\mathbf{H}^i, \mathbf{H}^i, \mathbf{H}^i)), \\ \mathbf{H}^{i+1} &= LN(\bar{\mathbf{H}}^i + FFN(\bar{\mathbf{H}}^i)), \\ MHA(\mathbf{H}^i, \mathbf{H}^i, \mathbf{H}^i) &= \mathbf{W}^O(\text{head}_1 || \dots || \text{head}_h), \\ \text{head}_i &= Attention(\mathbf{W}_i^Q \mathbf{H}^i, \mathbf{W}_i^K \mathbf{H}^i, \mathbf{W}_i^V \mathbf{H}^i), \\ Attention(\mathbf{H}^i, \mathbf{H}^i, \mathbf{H}^i) &= \text{softmax}\left(\frac{\mathbf{H}^i \mathbf{H}^{iT}}{\sqrt{d_k}}\right) \mathbf{H}^i, \\ FFN(\bar{\mathbf{H}}^i) &= \max(0, \mathbf{W}_1 \bar{\mathbf{H}}_P^{i+1} + \mathbf{b}_1) \mathbf{W}_2 + \mathbf{b}_2, \end{aligned} \quad (6)$$

where the range of i is from 1 to F , and $\mathbf{H}^1 = [\mathbf{H}^1 + \mathbf{P}\mathbf{E}_1, \mathbf{H}^2 + \mathbf{P}\mathbf{E}_2, \dots, \mathbf{H}^N + \mathbf{P}\mathbf{E}_N]$. $\mathbf{P}\mathbf{E}_i$ represent the positional encoding. $\bar{\mathbf{H}}^i$ represents the intermediate representation of the L_i layer after applying the frozen multi-head attention mechanism (MHA) and the first unfrozen layer normalization (LN). \mathbf{H}^i symbolizes the final representation of the L_i layer after applying both the unfrozen LN and frozen feed-forward network (FFN).

In the last U layers of the LLM, we unfreeze the *MHA* to adapt the ST-LLM for capturing spatial-temporal dependencies of traffic data:

$$\begin{aligned} \bar{\mathbf{H}}^{F+U-1} &= LN(\mathbf{H}^{F+U-1} + MHA(\mathbf{H}^{F+U-1}, \mathbf{H}^{F+U-1}, \mathbf{H}^{F+U-1})), \\ \mathbf{H}^{F+U} &= LN(\bar{\mathbf{H}}^{F+U-1} + FFN(\bar{\mathbf{H}}^{F+U-1})), \end{aligned} \quad (7)$$

where $\bar{\mathbf{H}}^{F+U}$ represents the intermediate representation of the L_{F+U-1} layer after applying the unfrozen MHA and the second frozen LN. \mathbf{H}^{F+U} denotes the final output of the L_{F+U} layer after applying both the unfrozen LN and frozen FFN, with the MHA being unfrozen.

After the PFA LLM, we design a regression convolution (RConv) to predict the traffic features on the following S timesteps:

$$\hat{\mathbf{Y}}_S = RConv(\mathbf{H}^{F+U}; \theta_r), \quad (8)$$

where $\hat{\mathbf{Y}}_S \in \mathbb{R}^{S \times N \times C}$, and θ_r represents the learnable parameters of the regression convolution.

The loss function of ST-LLM is established as follows:

$$\mathcal{L} = \|\hat{\mathbf{Y}}_S - \mathbf{Y}_S\| + \lambda \cdot L_{reg}, \quad (9)$$

where $\hat{\mathbf{Y}}_S$ is the predicted traffic feature. \mathbf{Y}_S is the ground truth. L_{reg} represents the L2 regularization term, which helps control overfitting. λ is a hyperparameter.

5 Experiments

5.1 Datasets

This section details the datasets employed to examine the predictive performance of the ST-LLM and baselines, with real-world traffic data from NYCTaxi [Ye *et al.*, 2021], CHBike [Jiang *et al.*, 2023].

NYCTaxi. The NYCTaxi dataset comprises over 35 million taxi trips in New York City (NYC), systematically categorized into 266 virtual stations. Spanning three months from

Table 1: Model comparison on NYCTaxi and CHBike datasets in terms of MAE, RMSE, MAPE (%), and WAPE (%).

Dataset Metric	NYCTaxi Pick-up				NYCTaxi Drop-off				CHBike Pick-up				CHBike Drop-off			
	MAE	RMSE	MAPE	WAPE	MAE	RMSE	MAPE	WAPE	MAE	RMSE	MAPE	WAPE	MAE	RMSE	MAPE	WAPE
DCRNN	5.40	9.71	35.09%	20.43%	5.19	9.63	37.78%	19.82%	2.09	3.30	54.22%	42.26%	1.96	2.94	51.42%	39.61%
STGCN	5.71	10.22	36.51%	21.62%	5.38	9.60	39.12%	20.55%	2.08	3.31	53.63%	42.08%	2.01	3.07	50.45%	40.62%
ASTGCN	7.43	13.84	47.96%	28.04%	6.98	14.70	45.48%	26.60%	2.76	4.45	64.23%	55.71%	2.79	4.20	69.88%	56.49%
GWN	5.43	9.39	37.79%	20.55%	5.03	8.78	35.63%	19.21%	2.04	3.20	53.08%	40.95%	1.95	2.98	50.30%	39.43%
AGCRN	5.79	10.11	40.40%	21.93%	5.45	9.56	40.67%	20.81%	2.16	3.46	56.35%	43.69%	2.06	3.19	51.91%	41.78%
GMAN	5.43	9.47	34.39%	20.42%	5.09	8.95	35.00%	19.33%	2.20	3.35	57.34%	44.06%	2.09	3.00	54.82%	42.00%
ASTGNN	5.90	10.71	40.15%	22.32%	6.28	12.00	49.78%	23.97%	2.37	3.67	60.08%	47.81%	2.24	3.35	57.21%	45.27%
STG-NCDE	6.24	11.25	43.20%	23.46%	5.38	9.74	40.45%	21.37%	2.15	3.97	55.49%	61.38%	2.28	3.42	60.96%	46.06%
DGCRN	5.44	9.82	35.78%	20.58%	5.14	9.39	35.09%	19.64%	2.06	3.21	54.06%	41.51%	1.96	2.93	51.99%	39.70%
OFA	5.82	10.42	36.67%	22.00%	5.60	10.14	37.39%	21.36%	2.06	3.21	53.55%	41.70%	1.96	2.97	49.64%	39.68%
GATGPT	5.92	10.55	37.83%	22.39%	5.66	10.39	37.36%	21.60%	2.07	3.23	52.54%	41.70%	1.95	2.94	49.26%	39.43%
GCNGPT	6.58	12.23	40.19%	24.88%	6.64	12.24	42.46%	25.32%	2.37	3.80	56.24%	47.66%	2.24	3.48	51.05%	45.37%
LLAMA2	5.35	9.48	41.32%	20.27%	5.66	10.74	47.47%	21.63%	2.10	3.37	56.63%	42.49%	1.99	3.03	55.23%	40.28%
ST-LLM	5.29	9.42	33.55%	20.03%	5.07	9.07	33.34%	19.18%	1.99	3.08	53.54%	40.19%	1.89	2.81	49.50%	38.27%

April 1st to June 30th, 2016, it includes 4,368 timesteps, each representing a half-hour interval.

CHBike. Consisting of approximately 2.6 million Citi bike orders, the CHBike dataset reflects the usage of the bike-sharing system in the same period as the NYCTaxi dataset, from April 1st to June 30th, 2016. After filtering out stations with few orders, it focuses on the 250 most frequented stations. The dataset aligns with NYCTaxi in terms of time, covering 4,368 timesteps with each timestep representing a 30-minute interval.

5.2 Baselines

We compare our ST-LLM with the following baseline models, which cover different types of methods and have been widely used for spatio-temporal prediction tasks. We compare ST-LLM with the following 10 baselines belonging to two classes. (1) GNN-based models: DCRNN [Li *et al.*, 2018], STGCN [Yu *et al.*, 2018], GWN [Wu *et al.*, 2019], AGCRN [Bai *et al.*, 2020], STG-NCDE [Choi *et al.*, 2022], DGCRN [Li *et al.*, 2023]. (2) Attention-based models: ASTGCN [Guo *et al.*, 2019], GMAN [Zheng *et al.*, 2020], ASTGNN [Guo *et al.*, 2022]. (3) LLM-based models: OFA [Zhou *et al.*, 2023], GATGPT [Chen *et al.*, 2023], GCNGPT, and LLAMA2.

5.3 Implementations

Aligning with contemporary practices, we divided the NYC-Taxi and CHBike datasets into training, validation, and test sets using a 6:2:2 ratio. We set the historical timesteps P and the future timesteps S to 12 each, enabling multi-step traffic prediction. T_w is set at 7 to represent a week’s seven days. T_d is 48, with each timestep spanning 30 minutes. The experiments were carried out on a system incorporating NVIDIA A100 GPUs, each with 40GB of memory. For training LLM-based models, we used the Ranger optimizer with a learning rate of 0.001, while GCN and attention-based models employed the Adam optimizer, also set at a 0.001 learning rate. The LLMs used are GPT2 and LLAMA2 7B. We configured GPT2 with six layers [Zhou *et al.*, 2023], and LLAMA2 with eight layers [Jin *et al.*, 2023b]. The experiments were conducted with a batch size of 64 over 200 training epochs. Note that the experimental results are averaged across all prediction timesteps.

5.4 Evaluation Metrics

Four metrics were used for evaluating the models: mean absolute error (MAE), mean absolute percentage error (MAPE), root mean squared error (RMSE), and weighted absolute percentage error (WAPE). MAE and RMSE quantify absolute errors, while MAPE and WAPE assess relative errors. In all metrics, lower values indicate superior prediction performance:

$$\text{MAE} = \frac{1}{m} \sum_{i=1}^m |\hat{\mathbf{Y}}_i - \mathbf{Y}_i|, \quad \text{MAPE} = \frac{100\%}{m} \sum_{i=1}^m \left| \frac{\hat{\mathbf{Y}}_i - \mathbf{Y}_i}{\mathbf{Y}_i} \right|, \quad (10)$$

$$\text{RMSE} = \sqrt{\frac{1}{m} \sum_{i=1}^m (\hat{\mathbf{Y}}_i - \mathbf{Y}_i)^2}, \quad \text{WAPE} = \frac{\sum_{i=1}^m |\hat{\mathbf{Y}}_i - \mathbf{Y}_i|}{\sum_{i=1}^m |\mathbf{Y}_i|} \times 100\%, \quad (11)$$

where m is the number of predicted values.

5.5 Results and Analysis

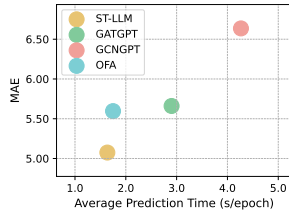
The comparison results with baselines are shown in Tables 1. We can make the following observations. (1) LLM-based methods yield superior prediction results, with ST-LLM exhibiting the most effective performance. The ST-LLM outperforms other LLMs in six traffic prediction scenarios, demonstrating its superior accuracy in handling diverse traffic data across various datasets. (2) OFA and LLAMA2 are competent but surpassed by ST-LLM which achieves a 22.5% average MAE improvement over OFA and 20.8% over LLAMA2. This may be due to OFA’s ineffective traffic data embedding, making it difficult for LLMs to understand the spatial-temporal dependencies between data. Despite LLAMA2’s larger size and complexity, it doesn’t directly translate to better traffic prediction than ST-LLM. GATGPT and GCNGPT do not extract temporal representations of traffic data to influence the LLM to capture spatial-temporal dependencies. (3) Attention-based models like ASTGNN and GMAN exhibit varied performance across different datasets. They performed quite well in some cases but were always inferior to ST-LLM. This variability could be attributed to the limitations of traditional attention mechanisms in handling complex spatial-temporal embeddings, especially when compared to large language models. (4) GNN-based Models such as GWN and DGCRN demonstrate competitive performance, particularly in specific metrics, but still cannot outperform ST-LLM.

Table 2: Ablation Study of Partially Frozen Attention LLM.

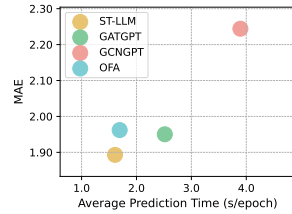
LLM	No Pretrain			Full Layer			Full Tuning			FPT			PFA		
	MAE	RMSE	WAPE	MAE	RMSE	WAPE	MAE	RMSE	WAPE	MAE	RMSE	WAPE	MAE	RMSE	WAPE
CHBike Drop-off	1.92	2.86	38.84%	1.91	2.83	38.63%	1.90	2.82	38.28%	1.92	2.86	38.90%	1.89	2.81	38.27%
CHBike Pick-up	2.03	3.14	40.87%	2.02	3.12	40.62%	2.01	3.11	40.43%	2.07	3.25	41.65%	1.99	3.08	40.19%

Table 3: Few-shot prediction results on 10% data of LLMs.

LLM	NYCTaxi Pick-up				NYCTaxi Drop-off				CHBike Pick-up				CHBike Drop-off			
	MAE	RMSE	MAPE	WAPE	MAE	RMSE	MAPE	WAPE	MAE	RMSE	MAPE	WAPE	MAE	RMSE	MAPE	WAPE
OFA	6.49	12.12	46.74%	24.54%	6.27	12.10	45.23%	23.92%	2.20	3.59	57.52%	44.40%	2.06	3.17	55.96%	41.63%
GATGPT	7.02	13.09	50.19%	26.54%	6.84	13.27	56.15%	26.09%	2.59	4.41	56.23%	52.20%	2.50	4.07	56.36%	50.64%
GCNGPT	10.31	18.82	59.41%	39.02%	9.25	19.50	56.77%	35.28%	2.73	4.44	56.93%	55.20%	2.79	4.65	61.85%	56.28%
LLAMA2	5.81	10.16	41.82%	21.99%	5.59	9.90	40.58%	21.35%	2.24	3.58	59.47%	45.20%	2.11	3.23	54.44%	42.75%
ST-LLM	5.40	9.63	33.36%	20.45%	5.54	9.84	39.56%	21.14%	2.07	3.23	55.68%	41.85%	1.93	2.88	52.75%	39.21%



(a) NYCTaxi Drop-off.



(b) CHBike Drop-off.

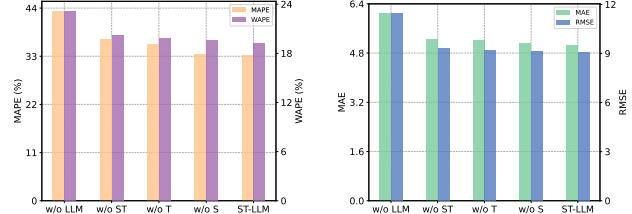
Figure 2: Inference time of LLMs.

This suggests that while GNNs effectively capture spatial dependencies, their temporal analysis capabilities might not be as advanced as the ST-LLM, which limits their overall performance.

Figure 2 illustrates the trade-off between inference time and MAE for various LLMs on NYCTaxi and CHBike Drop-off datasets. Notably, LLAMA2 is excluded from this comparison due to its substantially longer inference time relative to other LLMs. On the NYCTaxi Drop-off dataset, ST-LLM achieves the lowest MAE while maintaining competitive inference times. Following closely is OFA, whose inference time is similar to ST-LLM, albeit with a slightly higher MAE. This suggests that spatial-temporal embedding and PFA do not slow down the inference speed of the LLM, yet enhance prediction accuracy. GATGPT and GCNGPT exhibit longer inference times and higher MAEs than ST-LLM, with GCNGPT being the slowest. This could be attributed to the fact that while GCN generally has a simpler structure, their combination with GPT might introduce extra computational complexity. This also implies that GAT’s attention mechanism could be more efficient when combined with GPT. Similar trends are observed in the CHBike Drop-off dataset. In summary, ST-LLM stands out as the model providing the best balance between inference speed and predictive accuracy across both datasets.

5.6 Ablation Studies

With or Without Different Components. The ST-LLM’s effectiveness in traffic prediction stems from key components, explored through variant comparisons: w/o LLM (LLM removed), w/o ST (spatial-temporal embedding removed), w/o T (temporal embedding removed), and w/o S (spatial embedding removed). This analysis investigates the impact of each component. Figure 3 presents the ablation



(a) MAPE and WAPE.

(b) MAE and RMSE.

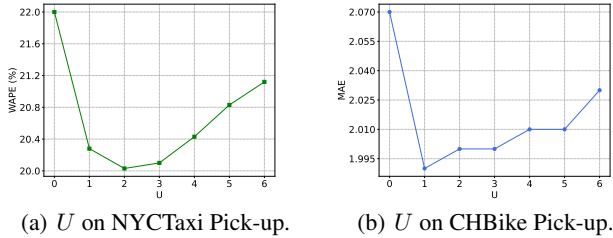
Figure 3: Ablation study of ST-LLM on NYCTaxi Drop-off dataset.

study on the NYCTaxi datasets. The w/o LLM variant shows a considerable increase in error across all metrics. Its removal leads to a degradation in performance, demonstrating that the prediction capabilities of the ST-LLM are heavily reliant on the LLM’s ability to learn complex dependencies from traffic data. The exclusion of ST results in a notable performance drop. This highlights the importance of spatial-temporal embedding in understanding both spatial and temporal dependencies in traffic data. The experimental results reveal that removing either temporal (w/o T) or spatial (w/o S) components similarly affects the model’s prediction error. Ablating either one of these embeddings results in an increased error. Notably, the model incurs a larger prediction error without the temporal component, underscoring the significance of our thoughtfully designed temporal embeddings.

Ablation Study of Partially Frozen Attention LLM. In this subsection, we conducted an ablation study to evaluate the efficacy of our proposed Partially Frozen Attention (PFA) LLM, as presented in Table 2. The PFA is compared against several variations: Frozen Pretrained Transformer (FPT), models without pretraining (No Pretrain), models utilizing the full 12 layers of GPT-2 (Full Layer), and fully tuned models without any frozen layers (Full Tuning). The PFA LLM demonstrates superior performance across all metrics on all datasets, which suggests that partially freezing the attention significantly enhances the predictive accuracy. FPT shows commendable performance, e.g., it is slightly outperformed by PFA. This indicates that the partial freezing strategy strikes a better balance between leveraging prelearned knowledge and adapting to new data. The Full Layer and Full Tuning models exhibit competitive performance. However, they still fall short of the accuracy demonstrated by the PFA model. The comparison with the No Pretrain model highlights the role of pretraining in model performance. While

Table 4: Zero-shot prediction results of LLMs.

LLM	OFA			GATGPT			GCNGPT			LLMAM2			ST-LLM		
	MAE	RMSE	MAPE	MAE	RMSE	MAPE	MAE	RMSE	MAPE	MAE	RMSE	MAPE	MAE	RMSE	MAPE
NYCTaxi Pick-up → CHBike Drop-off	3.57	5.72	59.26%	3.25	5.34	59.35%	3.49	5.64	59.06%	3.23	5.74	72.14%	3.12	5.01	55.12%
NYCTaxi Pick-up → CHBike Pick-up	3.61	5.98	59.55%	3.29	5.60	59.71%	3.53	5.91	59.14%	3.25	5.15	88.52%	3.06	5.40	50.94%
NYCTaxi Pick-up → NYCTaxi Drop-off	9.99	20.22	75.14%	10.00	21.16	68.03%	11.03	21.86	70.32%	11.02	22.34	94.31%	9.31	18.68	66.42%
NYCTaxi Drop-off → CHBike Drop-off	3.58	5.72	59.33%	3.19	4.99	76.75%	3.35	5.19	69.36%	3.29	4.99	80.87%	3.09	4.65	52.73%
NYCTaxi Drop-off → CHBike Pick-up	3.62	5.99	59.55%	3.26	5.27	79.41%	3.43	5.49	71.76%	3.33	5.32	82.60%	3.02	5.18	68.27%
NYCTaxi Drop-off → NYCTaxi Pick-up	10.04	17.72	88.10%	9.67	17.76	73.46%	8.09	14.58	50.99%	11.14	20.57	94.03%	8.02	13.21	46.16%

Figure 4: Performance study of unfreezing last U layers.

the No Pretrain model performs reasonably well, it is evident that pretraining, especially when combined with strategies like partial frozen is beneficial to achieving higher accuracy.

5.7 Parameter Analysis

Within the ST-LLM framework shown in Figure 4, U represents the hyperparameter that determines the number of multi-head attention layers to unfreeze during the training process. As depicted in Figure 4 (a), an analysis of the NYC-Taxi Pick-up dataset reveals that with an increase in U , the WAPE initially decreases. The trend suggests that unfreezing additional layers up to a certain threshold can enhance the performance of the ST-LLM. However, this positive effect inverts when U exceeds 2, at which point the model’s performance starts to degrade, hinting at the diminishing benefits associated with unfreezing more layers. In a nutshell, the optimal U of taxi flow prediction is set to 2. Figure 4 (b) illustrates a similar pattern on the CHBike Pick-up dataset. The MAE indicates an increase in performance as U is set to 1, with the lowest MAE observed at this value. This reinforces the observation that a single unfrozen multi-head attention layer is optimal for minimizing absolute errors, and the model achieves the balance between complexity and performance. This optimal point suggests that unfreezing more layers does not contribute to improved accuracy and might even degrade the performance of ST-LLM.

5.8 Few-Shot Prediction

In the few-shot prediction experiment, models trained with just 10% of data showed the ST-LLM model’s superior ability to recognize complex patterns from limited data, as detailed in Table 3. While the LLAMA2 model presents competitive results, especially on the NYCTaxi datasets, it does not consistently surpass the performance of ST-LLM. For instance, on the NYCTaxi pick-up dataset, ST-LLM achieves a noteworthy 7.06% reduction in MAE compared to LLAMA2. Other models, such as OFA, GATGPT, and GCNGPT, although commendable in their performances, do not match

the superior results of ST-LLM. Notably, despite OFA’s better performance on the CHBike Drop-off dataset, ST-LLM still outperforms it with a 9.15% improvement in MAE. Compared with GATGPT and GCNGPT, ST-LLM shows remarkable average improvements of over 39.21% and 7.80% in MAE across all datasets, respectively. This significant difference highlights the robustness of ST-LLM in efficiently handling scenarios with limited data.

5.9 Zero-Shot Prediction

This zero-shot prediction is designed to assess the cross-dataset adaptation capability of LLMs. This task evaluates the model’s ability to generalize to the CHBike dataset after being trained exclusively on the NYCTaxi dataset, without any prior exposure to data from the CHBike dataset. The results of this evaluation are shown in Table 4. In terms of intra-domain transfer (e.g., from NYCTaxi Pick-up to NYCTaxi Drop-off), ST-LLM demonstrates its ability to maintain high accuracy, underlining its effectiveness in handling dataset-specific dependencies. The results also show that ST-LLM exhibits exceptional performance in inter-domain scenarios, such as transferring from NYCTaxi to CHBike. This is evident in all metrics, where ST-LLM consistently achieves the lowest error rates, indicating a robust ability to adapt to new domains without retraining. When analyzing other LLMs like OFA, GATGPT, GCNGPT, and LLAMA2, we observe varied performances. For instance, OFA performs well in certain scenarios but is generally outperformed by ST-LLM. GATGPT and GCNGPT, while showing competent adaptability, still fall short compared to ST-LLM’s performance, particularly in challenging inter-domain transfers. In conclusion, the zero-shot prediction results reinforce the adaptability and predictive strength of ST-LLM, making it a highly promising model for traffic flow prediction tasks across diverse datasets.

6 Conclusion

ST-LLM shows promise in adapting large language models for traffic prediction by embedding traffic data into spatial-temporal representations for LLMs. A partially frozen attention strategy within ST-LLM is proposed to enhance the model in traffic prediction. Our research findings demonstrate that the ST-LLM outperforms state-of-the-art models in traffic prediction. Looking forward, future work will explore a range of additional tasks, such as traffic imputation, and will focus on developing memory-efficient LLMs tailored for traffic data analysis.

References

- [Bai *et al.*, 2020] Lei Bai, Lina Yao, Can Li, Xianzhi Wang, and Can Wang. Adaptive graph convolutional recurrent network for traffic forecasting. *Advances in neural information processing systems*, 33:17804–17815, 2020.
- [Campos *et al.*, 2023] David Campos, Miao Zhang, Bin Yang, Tung Kieu, Chenjuan Guo, and Christian S. Jensen. LightTS: Lightweight time series classification with adaptive ensemble distillation. *Proceedings of the ACM on Management of Data*, 1(2):171:1–171:27, 2023.
- [Cao *et al.*, 2023] Defu Cao, Furong Jia, Sercan O Arik, Tomas Pfister, Yixiang Zheng, Wen Ye, and Yan Liu. Tempo: Prompt-based generative pre-trained transformer for time series forecasting. *arXiv preprint arXiv:2310.04948*, 2023.
- [Chang *et al.*, 2023] Shih Yu Chang, Hsiao-Chun Wu, and Yi-Chih Kao. Tensor extended kalman filter and its application to traffic prediction. *IEEE Transactions on Intelligent Transportation Systems*, 24(12):13813–13829, 2023.
- [Chen *et al.*, 2023] Yakun Chen, Xianzhi Wang, and Guangdong Xu. Gatgpt: A pre-trained large language model with graph attention network for spatiotemporal imputation. *arXiv preprint arXiv:2311.14332*, 2023.
- [Choi *et al.*, 2022] Jeongwhan Choi, Hwangyong Choi, Jeehyun Hwang, and Noseong Park. Graph neural controlled differential equations for traffic forecasting. In *Thirty-Sixth Conference on Artificial Intelligence, Virtual Event, February 22 - March 1, 2022*.
- [Gong *et al.*, 2023] Jiahui Gong, Yu Liu, Tong Li, Haoye Chai, Xing Wang, Junlan Feng, Chao Deng, Depeng Jin, and Yong Li. Empowering spatial knowledge graph for mobile traffic prediction. In *Proceedings of the 31st ACM International Conference on Advances in Geographic Information Systems*, pages 1–11, 2023.
- [Guo *et al.*, 2019] Shengnan Guo, Youfang Lin, Ning Feng, Chao Song, and Huaiyu Wan. Attention based spatial-temporal graph convolutional networks for traffic flow forecasting. In *The Thirty-Third Conference on Artificial Intelligence, Honolulu, Hawaii, USA, January 27 - February 1*, pages 922–929, 2019.
- [Guo *et al.*, 2022] Shengnan Guo, Youfang Lin, Huaiyu Wan, Xiucheng Li, and Gao Cong. Learning dynamics and heterogeneity of spatial-temporal graph data for traffic forecasting. *IEEE Transactions on Knowledge and Data Engineering*, 34(11):5415–5428, 2022.
- [Ji *et al.*, 2023] Jiahao Ji, Jingyuan Wang, Chao Huang, Junjie Wu, Boren Xu, Zhenhe Wu, Junbo Zhang, and Yu Zheng. Spatio-temporal self-supervised learning for traffic flow prediction. In Brian Williams, Yiling Chen, and Jennifer Neville, editors, *Thirty-Seventh Conference on Artificial Intelligence, Washington, DC, USA, February 7-14*, pages 4356–4364, 2023.
- [Jiang *et al.*, 2023] Jiawei Jiang, Chengkai Han, Wayne Xin Zhao, and Jingyuan Wang. Pdformer: Propagation delay-aware dynamic long-range transformer for traffic flow prediction. In Brian Williams, Yiling Chen, and Jennifer Neville, editors, *Thirty-Seventh Conference on Artificial Intelligence, Washington, DC, USA, February 7-14*, pages 4365–4373, 2023.
- [Jin *et al.*, 2023a] Guangyin Jin, Yuxuan Liang, Yuchen Fang, Zezhi Shao, Jincui Huang, Junbo Zhang, and Yu Zheng. Spatio-temporal graph neural networks for predictive learning in urban computing: A survey. *IEEE Transactions on Knowledge and Data Engineering*, pages 1–20, 2023.
- [Jin *et al.*, 2023b] Ming Jin, Shiyu Wang, Lintao Ma, Zhixuan Chu, James Y Zhang, Xiaoming Shi, Pin-Yu Chen, Yuxuan Liang, Yuan-Fang Li, Shirui Pan, et al. Time-llm: Time series forecasting by reprogramming large language models. *International Conference on Learning Representations*, 2023.
- [Jin *et al.*, 2023c] Ming Jin, Qingsong Wen, Yuxuan Liang, Chaoli Zhang, Siqiao Xue, Xue Wang, James Zhang, Yi Wang, Haifeng Chen, Xiaoli Li, et al. Large models for time series and spatio-temporal data: A survey and outlook. *arXiv preprint arXiv:2310.10196*, 2023.
- [Ko *et al.*, 2023] Dohwan Ko, Joonmyung Choi, Hyeong Kyu Choi, Kyoung-Woon On, Byungseok Roh, and Hyunwoo J. Kim. MELTR: meta loss transformer for learning to fine-tune video foundation models. In *IEEE/CVF Conference on Computer Vision and Pattern Recognition, Vancouver, BC, Canada, June 17-24*, pages 20105–20115, 2023.
- [Kumar and Vanajakshi, 2015] S Vasantha Kumar and Lelitha Vanajakshi. Short-term traffic flow prediction using seasonal arima model with limited input data. *European Transport Research Review*, 7(3):1–9, 2015.
- [Lablack and Shen, 2023] Mourad Lablack and Yanming Shen. Spatio-temporal graph mixformer for traffic forecasting. *Expert Systems with Applications*, 228:120281, 2023.
- [Li *et al.*, 2018] Yaguang Li, Rose Yu, Cyrus Shahabi, and Yan Liu. Diffusion convolutional recurrent neural network: Data-driven traffic forecasting. In *International Conference on Learning Representations*, pages 1–16, 2018.
- [Li *et al.*, 2023] Fuxian Li, Jie Feng, Huan Yan, Guangyin Jin, Fan Yang, Funing Sun, Depeng Jin, and Yong Li. Dynamic graph convolutional recurrent network for traffic prediction: Benchmark and solution. *ACM Transactions on Knowledge Discovery from Data*, 17(1):9:1–9:21, 2023.
- [Lin *et al.*, 2020] Zhihui Lin, Maomao Li, Zhuobin Zheng, Yangyang Cheng, and Chun Yuan. Self-attention convlstm for spatiotemporal prediction. In *Thirty-Fourth Conference on Artificial Intelligence, New York, NY, USA, February 7-12*, pages 11531–11538, 2020.
- [Liu *et al.*, 2022a] Chenxi Liu, Zhu Xiao, Dong Wang, Minhao Cheng, Hongyang Chen, and Jiawei Cai. Foreseeing private car transfer between urban regions with multiple graph-based generative adversarial networks. *World Wide Web*, 25(6):2515–2534, 2022.

- [Liu *et al.*, 2022b] Chenxi Liu, Zhu Xiao, Dong Wang, Lei Wang, Hongbo Jiang, Hongyang Chen, and Jiangxia Yu. Exploiting spatiotemporal correlations of arrive-stay-leave behaviors for private car flow prediction. *IEEE Transactions on Network Science and Engineering*, 9(2):834–847, 2022.
- [Liu *et al.*, 2023a] Hangchen Liu, Zheng Dong, Renhe Jiang, Jiewen Deng, Jinliang Deng, Qunjun Chen, and Xuan Song. Spatio-temporal adaptive embedding makes vanilla transformer sota for traffic forecasting. In *Proceedings of the 32nd ACM International Conference on Information and Knowledge Management*, pages 4125–4129, 2023.
- [Liu *et al.*, 2023b] Yong Liu, Tengge Hu, Haoran Zhang, Haixu Wu, Shiyu Wang, Lintao Ma, and Mingsheng Long. itransformer: Inverted transformers are effective for time series forecasting. *arXiv preprint arXiv:2310.06625*, 2023.
- [Lu *et al.*, 2022] Kevin Lu, Aditya Grover, Pieter Abbeel, and Igor Mordatch. Frozen pretrained transformers as universal computation engines. In *Thirty-Sixth Conference on Artificial Intelligence, Virtual Event, February 22 - March 1*, pages 7628–7636, 2022.
- [Maynez *et al.*, 2023] Joshua Maynez, Priyanka Agrawal, and Sebastian Gehrmann. Benchmarking large language model capabilities for conditional generation. In Anna Rogers, Jordan L. Boyd-Graber, and Naoaki Okazaki, editors, *Proceedings of the 61st Annual Meeting of the Association for Computational Linguistics, Toronto, Canada, July 9-14*, pages 9194–9213, 2023.
- [Miao *et al.*, 2023] Hao Miao, Jiaying Shen, Jiannong Cao, Jiangnan Xia, and Senzhang Wang. Mba-stnet: Bayes-enhanced discriminative multi-task learning for flow prediction. *IEEE Trans. Knowl. Data Eng.*, 35(7):7164–7177, 2023.
- [Miao *et al.*, 2024] Hao Miao, Yan Zhao, Chenjuan Guo, Bin Yang, Zheng Kai, Feiteng Huang, Jiandong Xie, and Christian S. Jensen. A unified replay-based continuous learning framework for spatio-temporal prediction on streaming data. *IEEE International Conference on Data Engineering*, 2024.
- [Nate Gruver and Wilson, 2023] Shikai Qiu Nate Gruver, Marc Finzi and Andrew Gordon Wilson. Large language models are zero shot time series forecasters. In *Advances in Neural Information Processing Systems*, pages 1–29, 2023.
- [Ramezani and Xu, 2023] Aida Ramezani and Yang Xu. Knowledge of cultural moral norms in large language models. In Anna Rogers, Jordan L. Boyd-Graber, and Naoaki Okazaki, editors, *Proceedings of the 61st Annual Meeting of the Association for Computational Linguistics, Toronto, Canada, July 9-14*, pages 428–446, 2023.
- [Rasul *et al.*, 2023] Kashif Rasul, Arjun Ashok, Andrew Robert Williams, Arian Khorasani, George Adamopoulos, Rishika Bhagwatkar, Marin Biloš, Hena Ghonia, Nadhir Vincent Hassen, Anderson Schneider, et al. Lag-llama: Towards foundation models for time series forecasting. *arXiv preprint arXiv:2310.08278*, 2023.
- [Shao *et al.*, 2022] Zezhi Shao, Zhao Zhang, Wei Wei, Fei Wang, Yongjun Xu, Xin Cao, and Christian S. Jensen. Decoupled dynamic spatial-temporal graph neural network for traffic forecasting. *Proc. VLDB Endow.*, 15(11):2733–2746, jul 2022.
- [Shen *et al.*, 2018] Bilong Shen, Xiaodan Liang, Yufeng Ouyang, Miaofeng Liu, Weimin Zheng, and Kathleen M Carley. Stepdeep: A novel spatial-temporal mobility event prediction framework based on deep neural network. In *Proceedings of the 24th ACM SIGKDD international conference on knowledge discovery & data mining*, pages 724–733, 2018.
- [Song *et al.*, 2020] Chao Song, Youfang Lin, Shengnan Guo, and Huaiyu Wan. Spatial-temporal synchronous graph convolutional networks: A new framework for spatial-temporal network data forecasting. In *Proceedings of the AAAI conference on artificial intelligence*, volume 34, pages 914–921, 2020.
- [Sun *et al.*, 2023] Chenxi Sun, Yaliang Li, Hongyan Li, and Shenda Hong. Test: Text prototype aligned embedding to activate llm’s ability for time series. *arXiv preprint arXiv:2308.08241*, 2023.
- [Wang *et al.*, 2020] Senzhang Wang, Hao Miao, Hao Chen, and Zhiqiu Huang. Multi-task adversarial spatial-temporal networks for crowd flow prediction. In *Proceedings of the 29th ACM International Conference on Information & Knowledge Management*, page 1555–1564, 2020.
- [Wen *et al.*, 2023] Haomin Wen, Youfang Lin, Yutong Xia, Huaiyu Wan, Qingsong Wen, Roger Zimmermann, and Yuxuan Liang. Diffstg: Probabilistic spatio-temporal graph forecasting with denoising diffusion models. In *Proceedings of the 31st ACM International Conference on Advances in Geographic Information Systems*, pages 60:1–60:12, 2023.
- [Wu *et al.*, 2019] Zonghan Wu, Shirui Pan, Guodong Long, Jing Jiang, and Chengqi Zhang. Graph wavenet for deep spatial-temporal graph modeling. In Sarit Kraus, editor, *Proceedings of the Twenty-Eight International Joint Conference on Artificial Intelligence, Macao, China, August 10-16*, pages 1907–1913, 2019.
- [Wu *et al.*, 2023] Xinle Wu, Dalin Zhang, Miao Zhang, Chenjuan Guo, Bin Yang, and Christian S. Jensen. AutoCTS+: Joint neural architecture and hyperparameter search for correlated time series forecasting. *Proceedings of the ACM on Management of Data*, 1(1):97:1–97:26, 2023.
- [Xue *et al.*, 2022] Hao Xue, Bhanu Prakash Voutharoja, and Flora D. Salim. Leveraging language foundation models for human mobility forecasting. In *Proceedings of the 30th International Conference on Advances in Geographic Information Systems, Seattle, Washington, November 1-4*, pages 90:1–90:9, 2022.
- [Ye *et al.*, 2021] Junchen Ye, Leilei Sun, Bowen Du, Yanjie Fu, and Hui Xiong. Coupled layer-wise graph convolution

- for transportation demand prediction. In *Thirty-Fifth Conference on Artificial Intelligence, Virtual Event, February 2-9*, pages 4617–4625, 2021.
- [Yin *et al.*, 2021] Xueyan Yin, Genze Wu, Jinze Wei, Yanming Shen, Heng Qi, and Baocai Yin. Deep learning on traffic prediction: Methods, analysis, and future directions. *IEEE Transactions on Intelligent Transportation Systems*, 23(6):4927–4943, 2021.
- [Yu *et al.*, 2018] Bing Yu, Haoteng Yin, and Zhanxing Zhu. Spatio-temporal graph convolutional networks: A deep learning framework for traffic forecasting. In *Proceedings of the Twenty-Seven International Joint Conference on Artificial Intelligence*, page 3634–3640, 2018.
- [Yu *et al.*, 2023] Zhongzhi Yu, Shang Wu, Yonggan Fu, Shunyao Zhang, and Yingyan Celine Lin. Hint-aug: Drawing hints from foundation vision transformers towards boosted few-shot parameter-efficient tuning. In *IEEE/CVF Conference on Computer Vision and Pattern Recognition, Vancouver, BC, Canada, June 17-24*, pages 11102–11112, 2023.
- [Yuan *et al.*, 2018] Zhuoning Yuan, Xun Zhou, and Tianbao Yang. Hetero-convlstm: A deep learning approach to traffic accident prediction on heterogeneous spatio-temporal data. In *Proceedings of the 24th ACM SIGKDD international conference on knowledge discovery & data mining*, pages 984–992, 2018.
- [Zheng *et al.*, 2020] Chuanpan Zheng, Xiaoliang Fan, Cheng Wang, and Jianzhong Qi. Gman: A graph multi-attention network for traffic prediction. In *Proceedings of the AAAI conference on artificial intelligence*, volume 34, pages 1234–1241, 2020.
- [Zhou *et al.*, 2023] Tian Zhou, Peisong Niu, Xue Wang, Liang Sun, and Rong Jin. One Fits All: Power general time series analysis by pretrained lm. In *Advances in Neural Information Processing Systems*, pages 1–34, 2023.
- [Zhou *et al.*, 2024] Zhengyang Zhou, Jiahao Shi, Hongbo Zhang, Qiongyu Chen, Xu Wang, Hongyang Chen, and Yang Wang. Crest: A credible spatiotemporal learning framework for uncertainty-aware traffic forecasting. In *The 17th ACM International Conference on Web Search and Data Mining*, pages 1–10, 2024.